

Supplementary material for “A multimillennial Alpine ice core chronology synchronized with an accurately dated Arctic Pb record”

Paolo Gabrielli^{1,*}, Theo M. Jenk^{2,3,*}, Michele Bertó⁴, Giuliano Dreossi⁴, Daniela Festi⁵, Werner Kofler⁵,

5 Mai Winstrup⁶, Klaus Oegg⁵, Margit Schwikowski^{2,3,7}, Barbara Stenni⁴ and Carlo Barbante^{4,8}

¹Italian Glaciological Committee c/o University of Turin, Turin, Italy

²Center for Energy and Environmental Sciences, Paul Scherrer Institut, 5232 Villigen PSI, Switzerland

³Oeschger Centre for Climate Change Research, University of Bern, 3012 Bern, Switzerland

⁴Department of Environmental Sciences, Informatics and Statistics, Ca' Foscari University of Venice, Venice-Mestre, 30170,

10 Italy

⁵Institute for Botany, University of Innsbruck, Innsbruck, 6020, Austria

⁶DTU Space, Technical University of Denmark, Kongens Lyngby, 2800, Denmark

⁷Department of Chemistry and Biochemistry and Pharmaceutical Sciences, University of Bern, 3012 Bern, Switzerland

⁸Institute of Polar Sciences-CNR, Venice-Mestre, 30170, Italy

15 *Equally contributed to this manuscript

Correspondence to: Paolo Gabrielli (paologabrielli@hotmail.com), Theo Jenk (theo.jenk@psi.ch) and Carlo Barbante (barbante@unive.it)

Supplementary text 1: structure of the TC2016 chronology

The initial chronology, TC2016 (Gabielli et al., 2016), was developed by utilizing a common depth scale for Alto dell'Ortles cores #1, #2, and #3, using core #2 depth as a reference. Depth alignment of core #2 with #1 and with #3 was accomplished by matching common features in their $\delta^{18}\text{O}$ records (17 between #2 and #1, 14 between #2 and #3) (see Fig. 10 in Gabielli et al., 2016). This allowed the transfer of time markers in the cores to a common depth scale. Because of the lower resolution of the $\delta^{18}\text{O}$ record in core #3, only two match features, or “tie points”, could be established between cores #3 and #2 below 60 m depth. However, we realized later that this resulted in a depth misalignment of only few tens of cm, which nevertheless resulted in a significant time lag (up to ~300 years) between the 3 cores. This mismatch in depth and time became apparent by comparing two new high resolution Pb concentration records from cores #1 and #3 with TC2016 (see main text). The much larger Pb variability below 60 m depth, compared to the $\delta^{18}\text{O}$ variability, facilitated the detection of the initial mismatch of the isotope records in the ice cores.

Supplementary text 2: The Colle Gnifetti ice core timescale

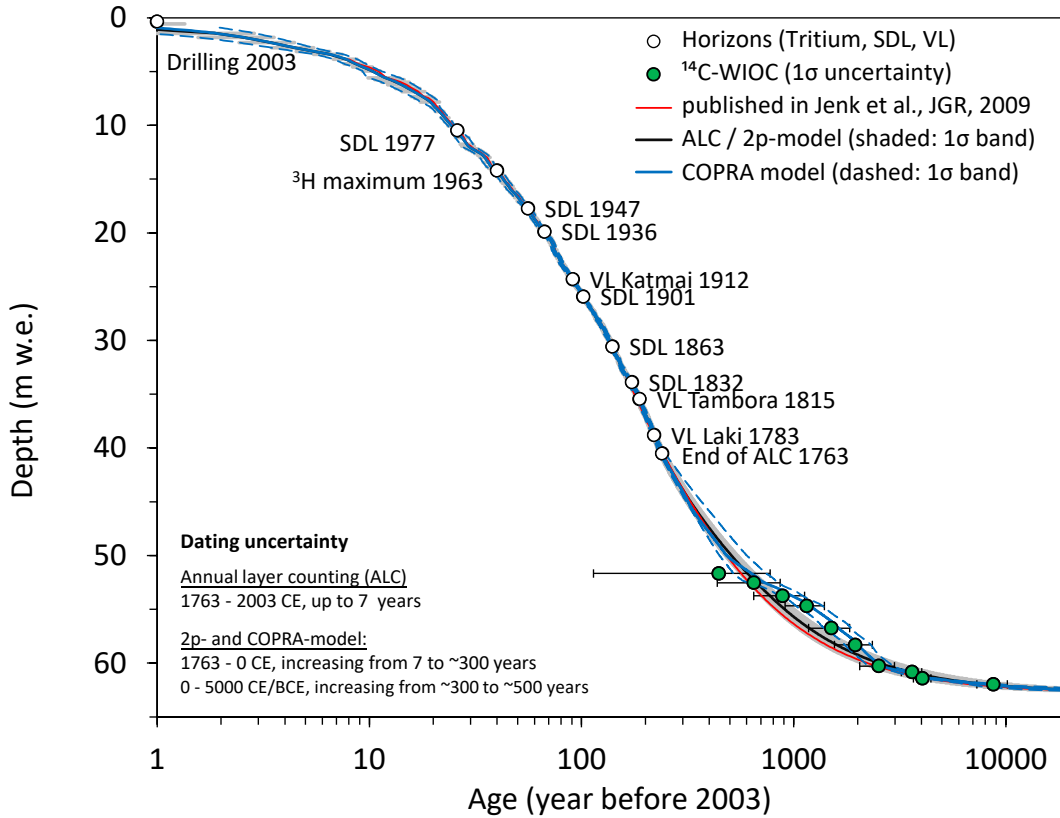
The Colle Gnifetti ice core (Mt. Rosa, Western Alps) is currently the oldest record from the Alps, dating back >15000
5 years (Jenk et al., 2009). The Colle Gnifetti Pb record was previously published by Schwikowski et al. (2004) and Gabrieli
and Barbante (2014). The chronology presented in the latter 2014 publication was based on the dating by Jenk et al. (2009).
Here, we take advantage of a revised dating of the Colle Gnifetti ice core (CG03B) and a Pb record from that core. Compared
to the timescale published by Jenk et al. (2009), CG03B (see details in Fig. S1) includes revisions in the counting of annual
layers (ALC) based on additional reference horizons of historical Sahara dust layers (SDL) and volcanic layers (VL) (Sigl et
10 al., 2018), as well as two additional ^{14}C -dates (Sigl et al., 2009). Thus, CG03B timescale is based on ALC (from 1763 to 2003
CE), a distinct ^3H peak, historical SDL and VL, and was independently confirmed by absolute dating with ^{210}Pb activity (Jenk
et al., 2009; Sigl et al., 2018). Before 1763 CE ages are modeled as an exponential equation constrained by ^{14}C -dates from the
measured water insoluble organic carbon (WIOC-14) fraction of carbonaceous particles (Jenk et al., 2009; Sigl et al., 2009),
assuming steady-state conditions and using a 1D ice flow model (2-parameter model, 2-p model) (Jenk et al., 2009). The
15 CG03B timescale has a relatively small uncertainty back to 1763 CE (up to a maximum of around ± 5 years) that increases
significantly to $\sim \pm 250$ years at the beginning of the record at ~ 350 CE. CG03B was previously used in Sigl et al. (2018) and
Brugger et al. (2021).

In figs. S2-3 we provide a comparison of the Colle Gnifetti non-crustal Pb concentration record with the
corresponding: i) the AN Arctic record which chronology was used as the reference time scale for the new dating of the Alto
20 dell'Ortles cores by synchronization (Fig. S2; see also main text); ii) recent portion of the Alto dell'Ortles record on the
CP2025/2 time scale (Fig S3). For the Colle Gnifetti core, the non-crustal Pb concentration record was obtained by using the
average crustal Pb/Ti ratio (0.00545 obtained from Wedepohl, 1995).

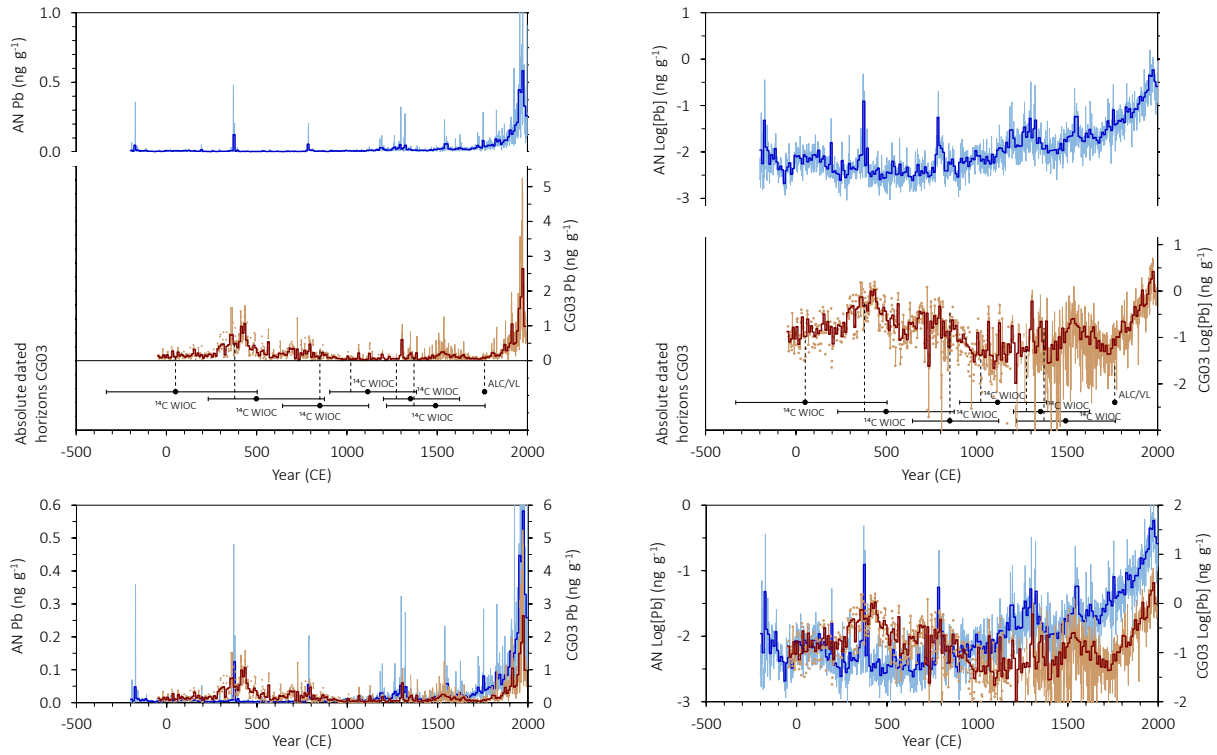
Supplementary text 3: Dansgaard-Johnsen (DJ) model framework

To understand our approach outlined in the main text, it is important to recognize that under the assumed steady-state conditions at the drill site, net annual snow accumulation (b , which in the accumulation zone equals the mass balance at that point; Cogley et al., 2011) and v_x along the glacier vertical profile are closely related. For reasons of mass conservation, if the amount of accumulated snow is not to increase the thickness of the glacier at that point, the same mass quantity must be removed from the ice column below. In more glaciological terms, the accumulated snow needs to be balanced by the horizontal strain and, due to the incompressibility of ice, the corresponding vertical strain rates (note the reduction to 1D, i.e., to the vertical axis). These fundamental principles are governed by the equation of continuity which, if integrated over the ice thickness, can also be written to relate to time and density (e.g., Whillans, 1977). In the DJ model, which considers these principles, the cumulative vertical strain of a layer at a certain depth over time (i.e., the total thinning) is related to the value of h . The DJ model accounts for the importance of density by using m w.e. as unit of length. This is essential, because in the firn section of the vertical column a substantial part of the horizontal stress will not cause deformation (i.e. the thinning governed by the model related to the incompressibility of ice), but instead enhances firn compaction by internal creep.

15

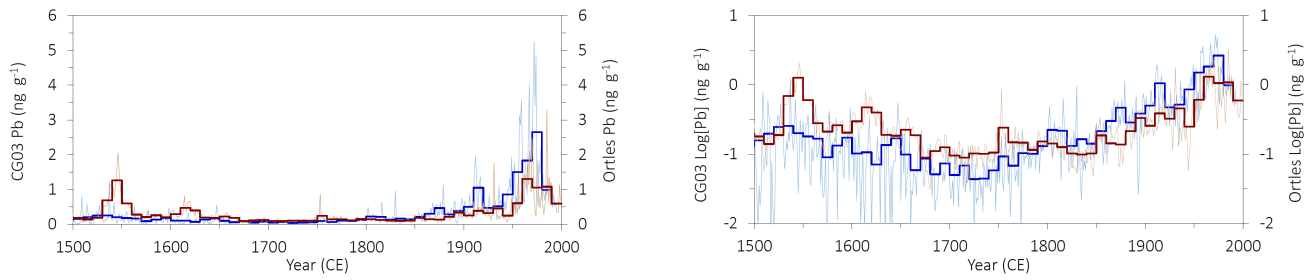


5 Figure S1: Dating of the Colle Gnifetti ice core (CG03B). Note the logarithmic age axis. This is a revised dating of Jenk et al. (2009) (red dashed line). This update also includes a revised counting of annual layers (ALC) based on additional reference horizons of historical Sahara dust layers (SDL) and volcanic layers (VL) (Sigl et al., 2018), as well as two additional ^{14}C -dates (Sigl et al., 2009). For details see supplementary text 2. Additionally shown here is the age scale derive by using the COPRA model in an exact same approach as used for the Alto dell'Ortles cores dating and using the time horizons indicated (blue lines).



5 Figure S2: Comparison of the non-crustal Pb concentrations from the Colle Gnifetti ice core (CG03; dark red) with the record from Akademii Nauk (AN; blue). Thin and thick lines show annual and 10-year averages, respectively. Absolute ages from ^{14}C dating (or ALC/VL) are shown at the bottom (dots indicate the μ -age and error bars the 1σ range), with the thick dashed line connecting to the record for visualizing the time horizons used to construct the CG03B time scale with COPRA (see supplementary text 2 and Fig. S1). Same for both panels, except for Pb concentrations being plotted on a logarithmic scale on the right panel. Bottom two panels with the Pb records shown in the upper panels being overlayed to facilitate visual comparison.

10



5

Figure S3: Comparison of the non-crustal Pb concentrations from Alto dell'Ortles #3 on CP2025/2 (Ortles; dark red) with the record from the Colle Gnifetti ice core (CG03; blue). Thin and thick lines show annual and 10-year averages, respectively. Same for both panels, except for Pb concentrations being plotted on a logarithmic scale on the right panel.

10

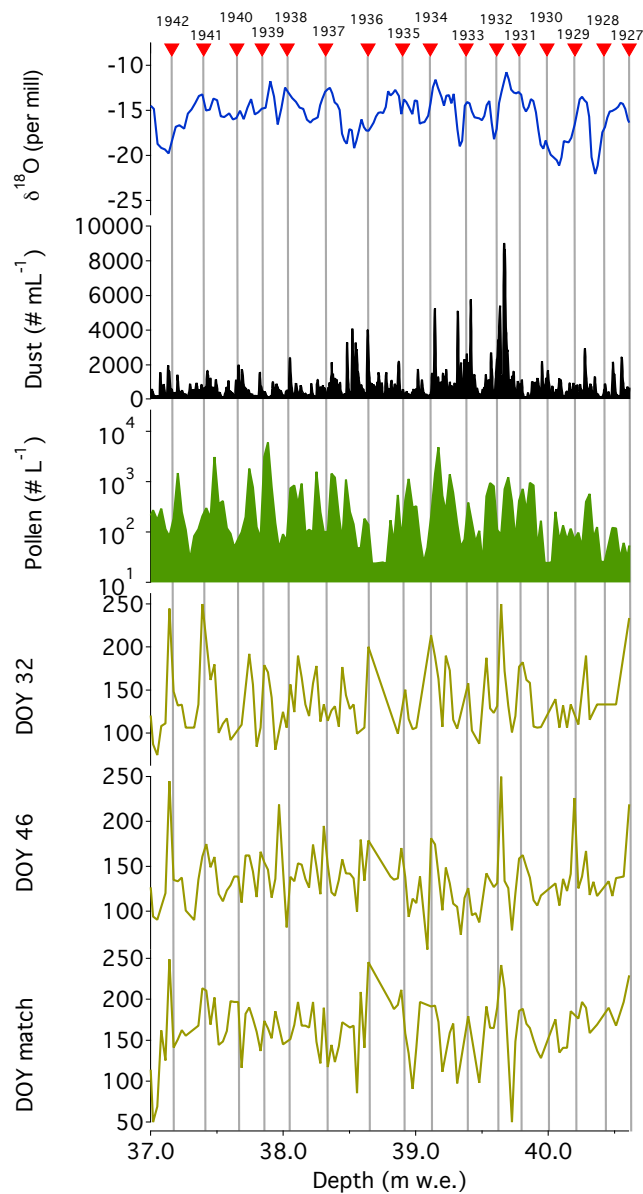


Figure S4: Annual layers between 37 and 41 m water equivalent (w.e.) in core #1 as shown by $\delta^{18}\text{O}$, dust and pollen concentrations, DOY 32 and 46 and DOY depth-to-day match (see main text).

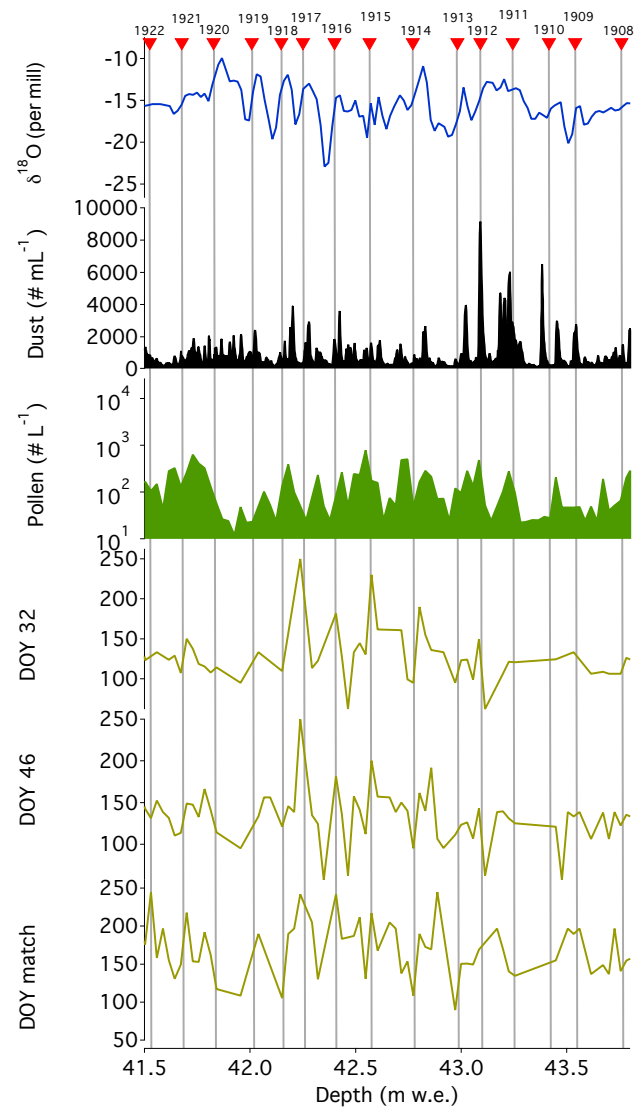


Figure S5: Annual layers between 41.5 and 43.5 m water equivalent (w.e.) in core #1 as shown by $\delta^{18}\text{O}$, dust and pollen concentrations, DOY 32 and 46 and DOY depth-to-day match (see main text).

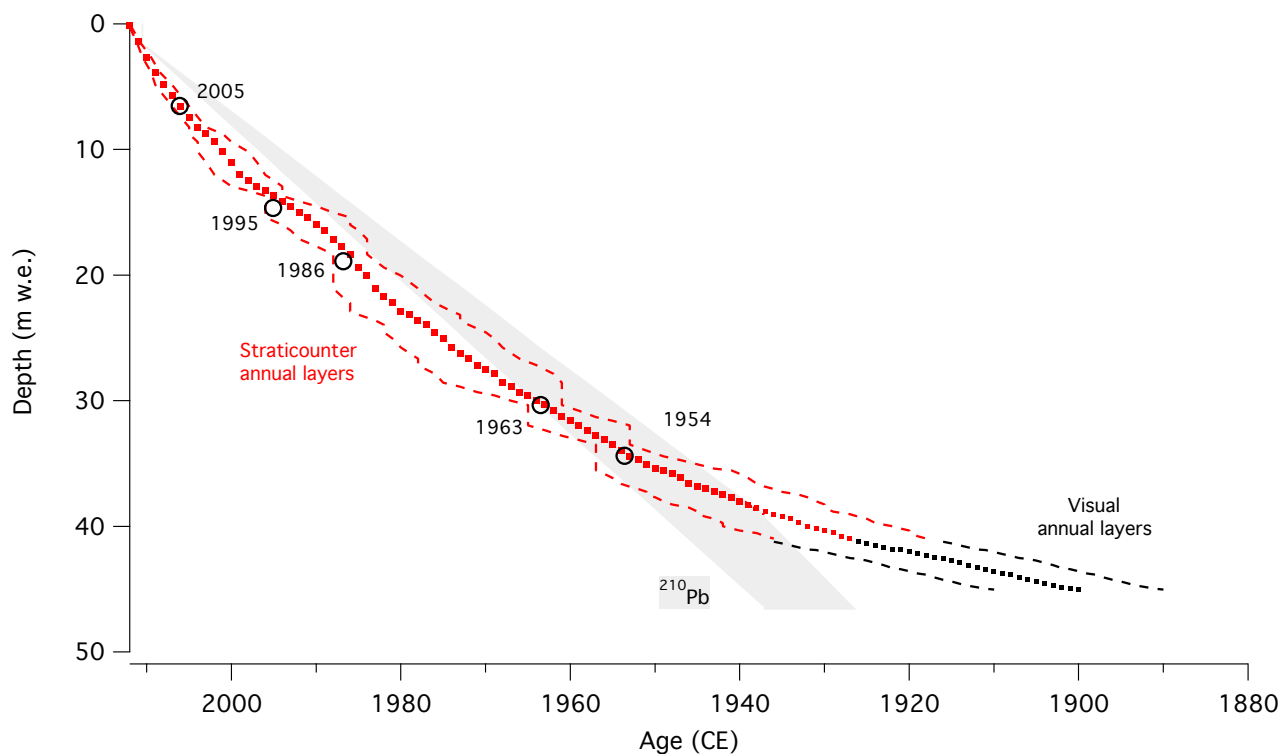


Figure S6: Comparison of the different time markers obtained in the shallow (recent) part of the Alto dell'Ortles cores. StratiCounter annual layer automatic counting (red dots; within 95% uncertainty) are superimposed on 5 fixed time markers (open circles; see also Table 3). ^{210}Pb ages from the TC2016 chronology are shown with uncertainty range (grey area; from Gabrielli et al., 2016). Annual layers are determined by visual counting (black dots within an assumed 10 years uncertainty).

Supplementary Table 1: Time markers used for the CP2025/1 timescale construction (part 1).

Depth in core #2 (m w.e.)	Age (yrsl2012)	Age uncertainty (years)	Type of time marker	Used in COPRA model
0.144	0.01	0.1	Annual layer (Stratocounter)	✓
1.435	1	0.2	Annual layer (Stratocounter)	✓
2.652	2	0.5	Annual layer (Stratocounter)	✓
3.843	3	0.5	Annual layer (Stratocounter)	✓
4.868	4	1	Annual layer (Stratocounter)	✓
5.713	5	1	Annual layer (Stratocounter)	✓
6.551	6	1	Annual layer (Stratocounter) and 2006 pollen peak	✓
7.404	7	1	Annual layer (Stratocounter)	✓
8.217	8	1	Annual layer (Stratocounter)	✓
8.761	9	2	Annual layer (Stratocounter)	✓
9.407	10	2	Annual layer (Stratocounter)	✓
10.182	11	3	Annual layer (Stratocounter)	✓
11.022	12	3	Annual layer (Stratocounter)	✓
12.017	13	3	Annual layer (Stratocounter)	✓
12.457	14	3	Annual layer (Stratocounter)	✓
12.931	15	3	Annual layer (Stratocounter)	✓
13.268	16	2	Annual layer (Stratocounter)	✓
13.687	17	1	Annual layer (Stratocounter) and 1995 pollen peak	✓
14.116	18	2	Annual layer (Stratocounter)	✓
14.509	19	3	Annual layer (Stratocounter)	✓
15.011	20	4	Annual layer (Stratocounter)	✓
15.402	21	5	Annual layer (Stratocounter)	✓
16.001	22	4	Annual layer (Stratocounter)	✓
16.454	23	4	Annual layer (Stratocounter)	✓
17.121	24	4	Annual layer (Stratocounter)	✓
17.712	25	3	Annual layer (Stratocounter)	✓
18.332	26	2	Annual layer (Stratocounter) and 1986 Beta peak	✓
19.395	27	3	Annual layer (Stratocounter)	✓
20.036	28	4	Annual layer (Stratocounter)	✓
21.048	29	5	Annual layer (Stratocounter)	✓
21.660	30	5	Annual layer (Stratocounter)	✓
22.223	31	5	Annual layer (Stratocounter)	✓
22.884	32	6	Annual layer (Stratocounter)	✓
23.162	33	6	Annual layer (Stratocounter)	✓
23.615	34	5	Annual layer (Stratocounter)	✓
23.952	35	5	Annual layer (Stratocounter)	✓
24.536	36	6	Annual layer (Stratocounter)	✓
25.043	37	6	Annual layer (Stratocounter)	✓
25.761	38	6	Annual layer (Stratocounter)	✓
26.200	39	6	Annual layer (Stratocounter)	✓
26.633	40	6	Annual layer (Stratocounter)	✓
27.166	41	7	Annual layer (Stratocounter)	✓
27.510	42	7	Annual layer (Stratocounter)	✓
27.849	43	7	Annual layer (Stratocounter)	✓
28.550	44	7	Annual layer (Stratocounter)	✓
28.880	45	6	Annual layer (Stratocounter)	✓
29.307	46	5	Annual layer (Stratocounter)	✓
29.573	47	4	Annual layer (Stratocounter)	✓
29.985	48	3	Annual layer (Stratocounter)	✓
30.327	49	2	Annual layer (Stratocounter) and 1963 tritium beta peaks	✓
30.802	50	3	Annual layer (Stratocounter)	✓
31.295	51	4	Annual layer (Stratocounter)	✓
31.599	52	5	Annual layer (Stratocounter)	✓
31.966	53	6	Annual layer (Stratocounter)	✓
32.334	54	5	Annual layer (Stratocounter)	✓
32.775	55	4	Annual layer (Stratocounter)	✓
33.118	56	3	Annual layer (Stratocounter)	✓
33.496	57	2	Annual layer (Stratocounter) and 1955 beta peak	✓
33.964	58	3	Annual layer (Stratocounter)	✓
34.427	59	4	Annual layer (Stratocounter)	✓
34.710	60	5	Annual layer (Stratocounter)	✓
35.061	61	6	Annual layer (Stratocounter)	✓
35.399	62	7	Annual layer (Stratocounter)	✓
35.549	63	8	Annual layer (Stratocounter)	✓

Supplementary Table 1: Time markers used for the CP2025/1 timescale construction (part 2).

Depth in core #2 (m w.e.)	Age (yrSB2012)	Age uncertainty (years)	Type of time marker	Used in COPRA model
35.819	64	8	Annual layer (Stratcounter)	✓
36.153	65	8	Annual layer (Stratcounter)	✓
36.603	66	8	Annual layer (Stratcounter)	✓
36.831	67	8	Annual layer (Stratcounter)	✓
37.014	68	8	Annual layer (Stratcounter)	✓
37.252	69	8	Annual layer (Stratcounter)	✓
37.468	70	9	Annual layer (Stratcounter)	✓
37.675	71	9	Annual layer (Stratcounter)	✓
38.002	72	9	Annual layer (Stratcounter)	✓
38.244	73	9	Annual layer (Stratcounter)	✓
38.503	74	8	Annual layer (Stratcounter)	✓
38.819	75	8	Annual layer (Stratcounter)	✓
39.020	76	9	Annual layer (Stratcounter)	✓
39.227	77	9	Annual layer (Stratcounter)	✓
39.391	78	9	Annual layer (Stratcounter)	✓
39.739	79	9	Annual layer (Stratcounter)	✓
39.977	80	10	Annual layer (Stratcounter)	✓
40.171	81	10	Annual layer (Stratcounter)	✓
40.329	82	10	Annual layer (Stratcounter)	✓
40.533	83	9	Annual layer (Stratcounter)	✓
40.796	84	9	Annual layer (Stratcounter)	✓
40.966	85	9	Annual layer (Stratcounter)	✓
41.227	86	10	Annual layer (Stratcounter)	✓
41.354	87	10	Annual layer (Stratcounter)	✓
41.509	88	10	Annual layer (Stratcounter)	✓
41.677	89	10	Annual layer (Stratcounter)	✓
41.834	90	10	Annual layer (Stratcounter)	✓
41.885	91	10	Annual layer (Stratcounter)	✓
42.037	92	10	Annual layer (Stratcounter)	✓
42.188	93	10	Annual layer (Stratcounter)	✓
42.367	94	10	Annual layer (Stratcounter)	✓
42.511	95	10	Annual layer (Stratcounter)	✓
42.595	96	10	Annual layer (Stratcounter)	✓
42.732	97	10	Annual layer (Stratcounter)	✓
42.911	98	10	Annual layer (Stratcounter)	✓
43.092	99	10	Annual layer (Stratcounter)	✓
43.311	100	10	Annual layer (Stratcounter)	✓
43.410	101	10	Annual layer (Stratcounter)	✓
43.566	102	10	Annual layer (Stratcounter)	✓
43.739	103	10	Annual layer (Stratcounter)	✓
43.851	104	10	Annual layer (Stratcounter)	✓
44.061	105	10	Annual layer (Stratcounter)	✓
44.247	106	10	Annual layer (Stratcounter)	✓
44.397	107	10	Annual layer (Stratcounter)	✓
44.569	108	10	Annual layer (Stratcounter)	✓
44.728	109	10	Annual layer (Stratcounter)	✓
44.836	110	10	Annual layer (Stratcounter)	✓
44.951	111	10	Annual layer (Stratcounter)	✓
45.023	112	10	Annual layer (Stratcounter)	✓
49.332	257	20	Pb tie point with SZ core	✓
51.070	337	20	Pb tie point with SZ core	✓
51.568	387	20	Pb tie point with SZ core	✓
52.482	467	20	Pb tie point with SZ core	✓
54.652	717	40	Pb tie point with SZ core	✓
55.243	651	204	¹⁴ C of bulk (WIOC)	X
56.203	1117	60	Pb tie point with SZ core	✓
57.045	1277	50	Pb tie point with SZ core	✓
58.110	1637	30	Pb tie point with SZ core	✓
58.295	1767	50	Pb tie point with SZ core	✓
58.433	1570	288	¹⁴ C of bulk (WIOC)	X
58.850	2244	126	¹⁴ C of macrofragment	X
58.994	2077	40	Pb tie point with SZ core	✓
59.107	2187	30	Pb tie point with SZ core	✓
59.470	2671	102	¹⁴ C of macrofragment	✓
60.288	4233	524	¹⁴ C of bulk (WIOC)	✓
60.510	5238	531	¹⁴ C of bulk (WIOC)	✓
60.712	6801	364	¹⁴ C of bulk (WIOC)	✓

Supplementary Table 2: Time markers used for the and CP2025/2 timescale construction (part 1).

Depth in core #2 (m w.e.)	Age (yrSB2012)	Age uncertainty (years)	Type of time marker	Used in COPRA model
0.144	0.01	0.1	Annual layer (Stratcounter)	✓
1.435	1	0.2	Annual layer (Stratcounter)	✓
2.652	2	0.5	Annual layer (Stratcounter)	✓
3.843	3	0.5	Annual layer (Stratcounter)	✓
4.868	4	1	Annual layer (Stratcounter)	✓
5.713	5	1	Annual layer (Stratcounter)	✓
6.551	6	1	Annual layer (Stratcounter) and 2006 pollen peak	✓
7.404	7	1	Annual layer (Stratcounter)	✓
8.217	8	1	Annual layer (Stratcounter)	✓
8.761	9	2	Annual layer (Stratcounter)	✓
9.407	10	2	Annual layer (Stratcounter)	✓
10.182	11	3	Annual layer (Stratcounter)	✓
11.022	12	3	Annual layer (Stratcounter)	✓
12.017	13	3	Annual layer (Stratcounter)	✓
12.457	14	3	Annual layer (Stratcounter)	✓
12.931	15	3	Annual layer (Stratcounter)	✓
13.268	16	2	Annual layer (Stratcounter)	✓
13.687	17	1	Annual layer (Stratcounter) and 1995 pollen peak	✓
14.116	18	2	Annual layer (Stratcounter)	✓
14.509	19	3	Annual layer (Stratcounter)	✓
15.011	20	4	Annual layer (Stratcounter)	✓
15.402	21	5	Annual layer (Stratcounter)	✓
16.001	22	4	Annual layer (Stratcounter)	✓
16.454	23	4	Annual layer (Stratcounter)	✓
17.121	24	4	Annual layer (Stratcounter)	✓
17.712	25	3	Annual layer (Stratcounter)	✓
18.332	26	2	Annual layer (Stratcounter) and 1986 Beta peak	✓
19.395	27	3	Annual layer (Stratcounter)	✓
20.036	28	4	Annual layer (Stratcounter)	✓
21.048	29	5	Annual layer (Stratcounter)	✓
21.660	30	5	Annual layer (Stratcounter)	✓
22.223	31	5	Annual layer (Stratcounter)	✓
22.884	32	6	Annual layer (Stratcounter)	✓
23.162	33	6	Annual layer (Stratcounter)	✓
23.615	34	5	Annual layer (Stratcounter)	✓
23.952	35	5	Annual layer (Stratcounter)	✓
24.536	36	6	Annual layer (Stratcounter)	✓
25.043	37	6	Annual layer (Stratcounter)	✓
25.761	38	6	Annual layer (Stratcounter)	✓
26.200	39	6	Annual layer (Stratcounter)	✓
26.633	40	6	Annual layer (Stratcounter)	✓
27.166	41	7	Annual layer (Stratcounter)	✓
27.510	42	7	Annual layer (Stratcounter)	✓
27.849	43	7	Annual layer (Stratcounter)	✓
28.550	44	7	Annual layer (Stratcounter)	✓
28.880	45	6	Annual layer (Stratcounter)	✓
29.307	46	5	Annual layer (Stratcounter)	✓
29.573	47	4	Annual layer (Stratcounter)	✓
29.985	48	3	Annual layer (Stratcounter)	✓
30.327	49	2	Annual layer (Stratcounter) and 1963 tritium beta peaks	✓
30.802	50	3	Annual layer (Stratcounter)	✓
31.295	51	4	Annual layer (Stratcounter)	✓
31.599	52	5	Annual layer (Stratcounter)	✓
31.966	53	6	Annual layer (Stratcounter)	✓
32.334	54	5	Annual layer (Stratcounter)	✓
32.775	55	4	Annual layer (Stratcounter)	✓
33.118	56	3	Annual layer (Stratcounter)	✓
33.496	57	2	Annual layer (Stratcounter) and 1955 beta peak	✓
33.964	58	3	Annual layer (Stratcounter)	✓
34.427	59	4	Annual layer (Stratcounter)	✓
34.710	60	5	Annual layer (Stratcounter)	✓
35.061	61	6	Annual layer (Stratcounter)	✓
35.399	62	7	Annual layer (Stratcounter)	✓
35.549	63	8	Annual layer (Stratcounter)	✓

Supplementary Table 2: Time markers used for the and CP2025/2 timescale construction (part 2).

Depth in core #2 (m w.e.)	Age (yrSB2012)	Age uncertainty (years)	Type of time marker	Used in COPRA model
35.819	64	8	Annual layer (Stratocounter)	✓
36.153	65	8	Annual layer (Stratocounter)	✓
36.603	66	8	Annual layer (Stratocounter)	✓
36.831	67	8	Annual layer (Stratocounter)	✓
37.014	68	8	Annual layer (Stratocounter)	✓
37.252	69	8	Annual layer (Stratocounter)	✓
37.468	70	9	Annual layer (Stratocounter)	✓
37.675	71	9	Annual layer (Stratocounter)	✓
38.002	72	9	Annual layer (Stratocounter)	✓
38.244	73	9	Annual layer (Stratocounter)	✓
38.503	74	8	Annual layer (Stratocounter)	✓
38.819	75	8	Annual layer (Stratocounter)	✓
39.020	76	9	Annual layer (Stratocounter)	✓
39.227	77	9	Annual layer (Stratocounter)	✓
39.391	78	9	Annual layer (Stratocounter)	✓
39.739	79	9	Annual layer (Stratocounter)	✓
39.977	80	10	Annual layer (Stratocounter)	✓
40.171	81	10	Annual layer (Stratocounter)	✓
40.329	82	10	Annual layer (Stratocounter)	✓
40.533	83	9	Annual layer (Stratocounter)	✓
40.796	84	9	Annual layer (Stratocounter)	✓
40.966	85	9	Annual layer (Stratocounter)	✓
41.227	86	10	Annual layer (Stratocounter)	✓
41.354	87	10	Annual layer (Stratocounter)	✓
41.509	88	10	Annual layer (Stratocounter)	✓
41.677	89	10	Annual layer (Stratocounter)	✓
41.834	90	10	Annual layer (Stratocounter)	✓
41.885	91	10	Annual layer (Stratocounter)	✓
42.037	92	10	Annual layer (Stratocounter)	✓
42.188	93	10	Annual layer (Stratocounter)	✓
42.367	94	10	Annual layer (Stratocounter)	✓
42.511	95	10	Annual layer (Stratocounter)	✓
42.595	96	10	Annual layer (Stratocounter)	✓
42.732	97	10	Annual layer (Stratocounter)	✓
42.911	98	10	Annual layer (Stratocounter)	✓
43.092	99	10	Annual layer (Stratocounter)	✓
43.311	100	10	Annual layer (Stratocounter)	✓
43.410	101	10	Annual layer (Stratocounter)	✓
43.566	102	10	Annual layer (Stratocounter)	✓
43.739	103	10	Annual layer (Stratocounter)	✓
43.851	104	10	Annual layer (Stratocounter)	✓
44.061	105	10	Annual layer (Stratocounter)	✓
44.247	106	10	Annual layer (Stratocounter)	✓
44.397	107	10	Annual layer (Stratocounter)	✓
44.569	108	10	Annual layer (Stratocounter)	✓
44.728	109	10	Annual layer (Stratocounter)	✓
44.836	110	10	Annual layer (Stratocounter)	✓
44.951	111	10	Annual layer (Stratocounter)	✓
45.023	112	10	Annual layer (Stratocounter)	✓
49.332	257	20	Pb tie point with SZ core	✓
51.070	337	20	Pb tie point with SZ core	✓
51.568	387	20	Pb tie point with SZ core	✓
52.482	467	20	Pb tie point with SZ core	✓
54.652	717	40	Pb tie point with SZ core	✓
55.243	651	204	¹⁴ C of bulk (WIOC)	X
56.203	1117	60	Pb tie point with SZ core	✓
57.045	1277	50	Pb tie point with SZ core	✓
58.110	1637	30	Pb tie point with SZ core	✓
58.295	1767	50	Pb tie point with SZ core	✓
58.433	1570	288	¹⁴ C of bulk (WIOC)	X
58.850	2244	126	¹⁴ C of macrofragment	X
58.994	2077	40	Pb tie point with SZ core	✓
59.107	2187	30	Pb tie point with SZ core	✓
59.470	2671	102	¹⁴ C of macrofragment	✓
60.288	4233	524	¹⁴ C of bulk (WIOC)	✓
60.510	5238	531	¹⁴ C of bulk (WIOC)	✓
60.712	6801	364	¹⁴ C of bulk (WIOC)	✓

Supplementary references

- 5 • Brugger, S. O., Schwikowski, M., Gobet, E., Schwörer, C., Rohr, C., Sigl, M., Henne, S., Pfister, C., Jenk, T. M., Henne, P. D., and Tinner, W.: Alpine Glacier Reveals Ecosystem Impacts of Europe's Prosperity and Peril Over the Last Millennium, *Geoph. Res. Let.*, 48, e2021GL095039, <https://doi.org/10.1029/2021GL095039>, 2021.
- 10 • Cogley, J. G., Hock, R., Rasmussen, L. A., Arendt, A. A., Bauder, A., Braithwaite, R. J., Jansson, P., Kaser, G., Möller, M., Nicholson, L., and Zemp, M.: Glossary of glacier mass balance and related term, UNESCO/IHP, Paris 2011.
- 15 • Gabrieli, J. and Barbante, C.: The Alps in the age of the Anthropocene: the impact of human activities on the cryosphere recorded in the Colle Gnifetti glacier, *Rend. Fis. Acc. Lincei*, 25, 71-83, 10.1007/s12210-014-0292-2, 2014.
- 20 • Gabrielli, P., Barbante, C., Bertagna, G., Bertó, M., Binder, D., Carton, A., Carturan, L., Cazorzi, F., Cozzi, G., Dalla Fontana, G., Davis, M., De Blasi, F., Dinale, R., Dragà, G., Dreossi, G., Festi, D., Frezzotti, M., Gabrieli, J., Galos, S., Ginot, P., Heidenwolf, P., Jenk, T. M., Kehrwald, N., Kenny, D., Magand, O., Mair, V., Mikhalenko, V. N., Lin, P. N., Oegg, K., Piffer, G., Rinaldi, M., Schotterer, U., Schwikowski, M., Seppi, R., Spolaor, A., Stenni, B., Tonidandel, D., Uglietti, C., Zagorodnov, V. S., Zanoner, T., and Zennaro, P.: Age of the Mt. Ortles ice cores, the Tyrolean Iceman and glaciation of the highest summit of South Tyrol since the Northern Hemisphere Climatic Optimum, *The Cryosphere*, 10, 2779–2797, 10.5194/tc-10-2779-2016, 2016.
- 25 • Jenk, T. M., Szidat, S., Bolius, D., Sigl, M., Gäggeler, H. W., Wacker, L., Ruff, M., Barbante, C., Boutron, C. F., and Schwikowski, M.: A novel radiocarbon dating technique applied to an ice core from the Alps indicating late Pleistocene ages *J. Geophys. Res. Atmos.*, 114, [10.1029/2009JD011860](https://doi.org/10.1029/2009JD011860), 2009.
- 30 • Schwikowski, M., Barbante, C., Doering, T., Gaeggeler, H. W., Boutron, C. F., Schotterer, U., Tobler, L., Van de Velde, K., Ferrari, C., Cozzi, G., Rosman, K., and Cescon, P.: Post-17th-century changes of European lead emissions recorded in high-altitude alpine snow and ice, *Environ. Sci. Technol.*, 38, 957-964, 2004.
- 35 • Sigl, M., Abram, N. J., Gabrieli, J., Jenk, T. M., Osmont, D., and Schwikowski, M.: 19th century glacier retreat in the Alps preceded the emergence of industrial black carbon deposition on high-alpine glaciers, *The Cryosphere*, 12, 3311-3331, 10.5194/tc-12-3311-2018, 2018.
- Sigl, M., Jenk, T. M., Kellerhals, T., Szidat, S., Gäggeler, H. W., Wacker, L., Synal, H. A., Boutron, C. F., Barbante, C., Gabrieli, J., and Schwikowski, M.: Instruments and methods: towards radiocarbon dating of ice cores, *J. Glaciol.*, 55, 985-996, 2009.
- Whillans, I. M.: The Equation of Continuity and its Application to the Ice Sheet Near “byrd” Station, Antarctica, *J. Glaciol.*, 18, 359-371, 10.3189/S0022143000021055, 1977.